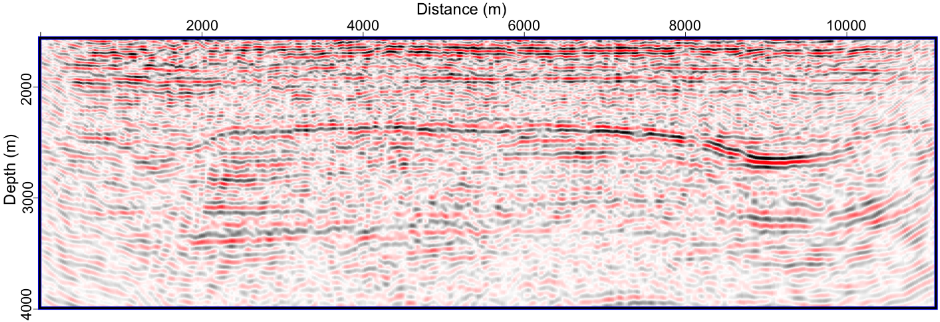
Distance (m)
2000
4000
6000
8000
10000
Depth (m)
2000
3000
4000

Time-lapse image

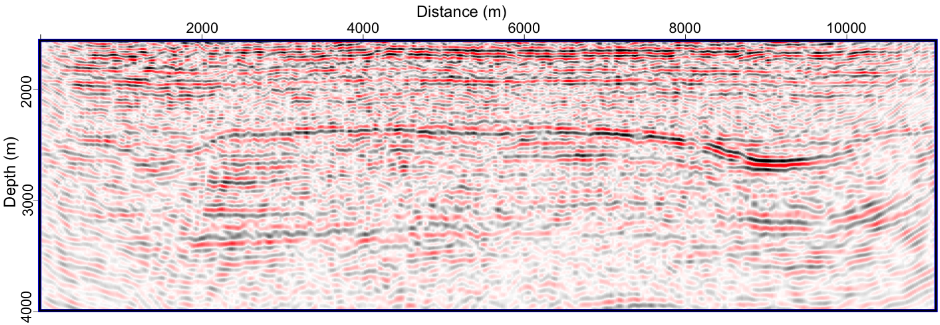

Time-lapse image: raw

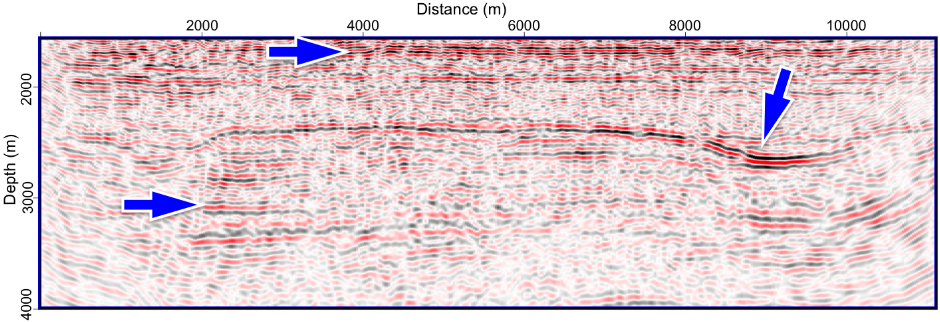

Time-lapse image: inverted

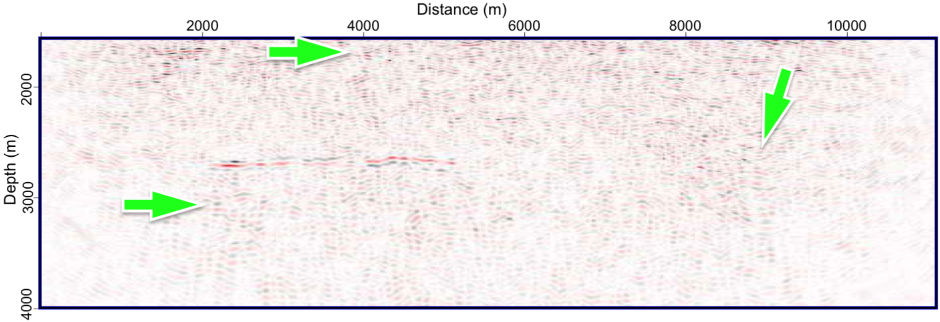

Time-lapse image: inverted

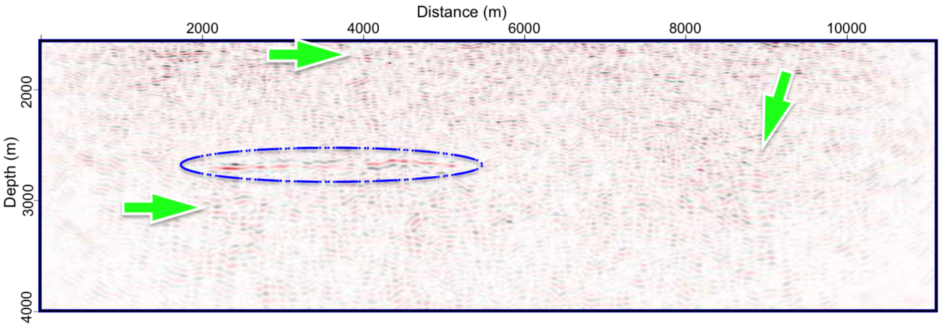

Time-lapse image: raw

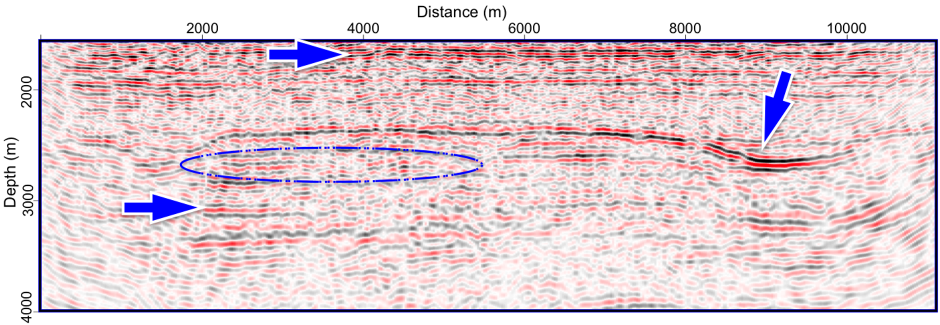

gayeni@sep.stanford.edu

Time-lapse image: raw+obstruction

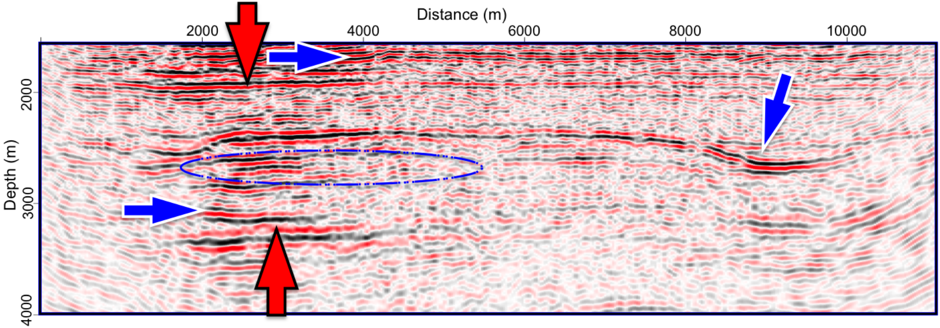

Wave-equation inversion of time-lapse seismic data sets

Gboyega Ayeni & Biondi Biondi

SEP 143: Pgs 119-136

SEP Sponsors' Meeting

June, 2011

Wave-equation inversion of time-lapse seismic data sets

Gboyega Ayeni & Biondi Biondi

SEP 143: Pgs 119-136

SEP Sponsors' Meeting

June, 2011

Time-lapse imaging – Acquisition

Baseline

$$\mathbf{L}_0\mathbf{m}_0 = \mathbf{d}_0$$

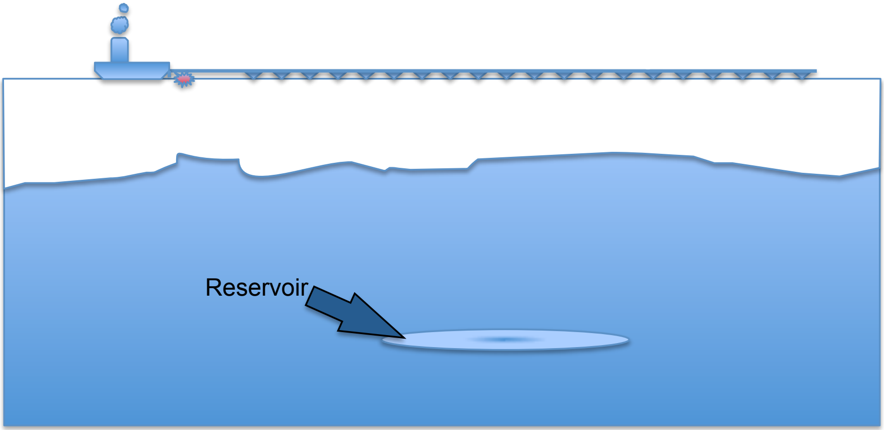

Time-lapse imaging – Acquisition

Monitor

$$\mathbf{L}_1\mathbf{m}_1 = \mathbf{d}_1$$

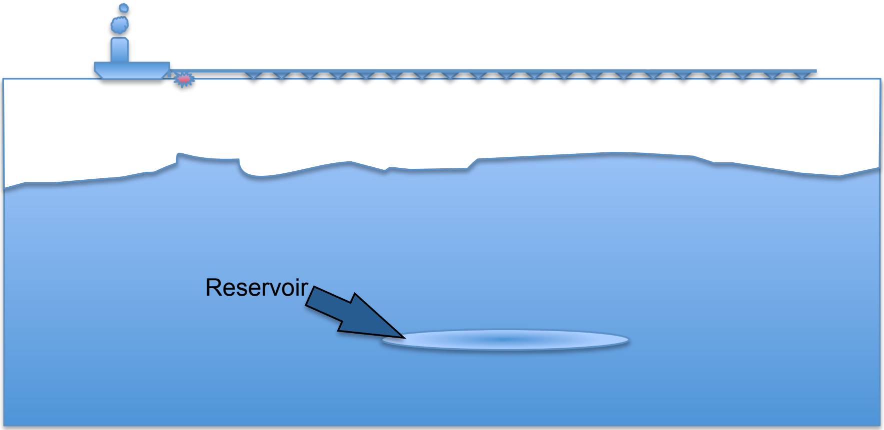

Time-lapse imaging

$$\mathbf{L}_0\mathbf{m}_0 = \mathbf{d}_0$$
$$\mathbf{L}_1\mathbf{m}_1 = \mathbf{d}_1$$

$$\Delta\mathbf{m} = \mathbf{m}_1 - \mathbf{m}_0$$

$\mathbf{L}_i$: modeling (acquisition) operator
$\mathbf{d}_i$: seismic data
$\mathbf{m}_i$: earth reflectivity model
$\Delta\mathbf{m}$: time-lapse image
$_{i=0}$: Baseline
$_{i=1}$: Monitor

gayeni@sep.stanford.edu

Time-lapse imaging

$$\mathbf{L}_0\mathbf{m}_0 = \mathbf{d}_0$$
$$\mathbf{L}_1\mathbf{m}_1 = \mathbf{d}_1$$

$$\Delta\mathbf{m} = \mathbf{m}_1 - \mathbf{m}_0$$
$$\Delta\tilde{\mathbf{m}} = \tilde{\mathbf{m}}_1 - \tilde{\mathbf{m}}_0$$

$\mathbf{L}_i$: modeling (acquisition) operator
$\mathbf{d}_i$: seismic data
$\mathbf{m}_i$: earth reflectivity model
$\Delta\mathbf{m}$: time-lapse image
$_{i=0}$: Baseline
$_{i=1}$: Monitor
$\tilde{\mathbf{m}}_i$: migrated image ($\mathbf{L}^{T}{}_i\mathbf{d}_i$)

gayeni@sep.stanford.edu

Key assumptions

- Production- (or injection-) related changes in acoustic properties are measurable
- The baseline migration velocity model is accurate

Key assumptions

- Production- (or injection-) related changes in acoustic properties are measurable
- The baseline migration velocity model is accurate
- Velocity changes between surveys are *small*

Key assumptions

- Production- (or injection-) related changes in acoustic properties are measurable
- The baseline migration velocity model is accurate
- Velocity changes between surveys are *small*
- Compaction and other geomechanical effects between surveys are *small*

Key assumptions

- Production- (or injection-) related changes in acoustic properties are measurable
- The baseline migration velocity model is accurate
- Velocity changes between surveys are *small*
- Compaction and other geomechanical effects between surveys are *small*
- Data comprise only primary reflections

Key assumptions

- Production- (or injection-) related changes in acoustic properties are measurable
- The baseline migration velocity model is accurate
- Velocity changes between surveys are *small*
- Compaction and other geomechanical effects between surveys are *small*
- Data comprise only primary reflections

gayeni@sep.stanford.edu

Key assumptions

- Production- (or injection-) related changes in acoustic properties are measurable
- The baseline migration velocity model is accurate
- Velocity changes between surveys are *small*
- Compaction and other geomechanical effects between surveys are *small*
- Data comprise only primary reflections

Workflow: 4D processing

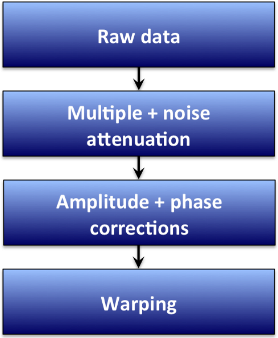

gayeni@sep.stanford.edu

Workflow: 4D processing

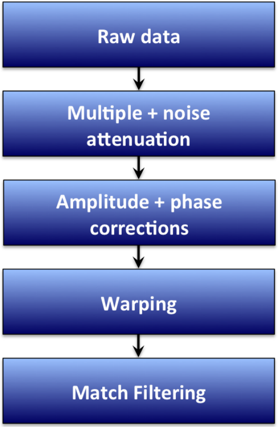

Workflow: 4D processing–updated

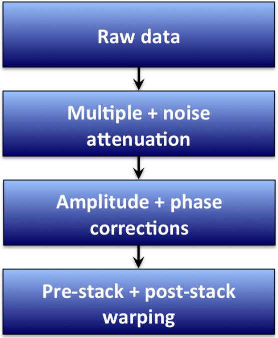

Workflow: 4D processing+inversion

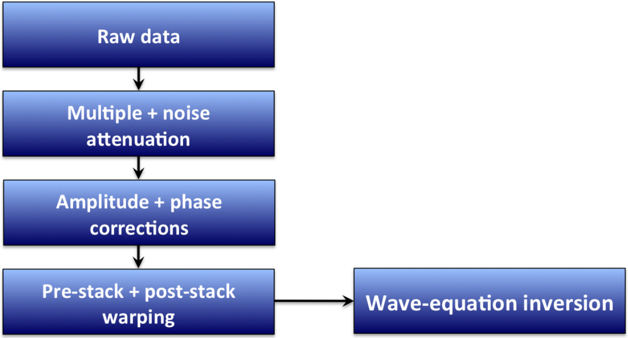

Workflow: 4D processing+inversion

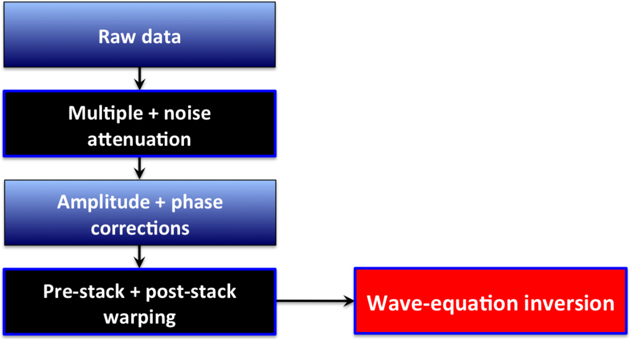

gayeni@sep.stanford.edu

Data-space inversion

$$\mathbf{L}_0\mathbf{m}_0 = \mathbf{d}_0$$
$$\mathbf{L}_1\mathbf{m}_1 = \mathbf{d}_1$$

$\mathbf{d}_i$ – data
$\mathbf{m}_i$ – reflectivity image
$\mathbf{L}_i$ – modeling operator
$\mathbf{\Delta m}$ – time-lapse image

gayeni@sep.stanford.edu

Data-space inversion

$$\left\| \begin{bmatrix} \mathbf{L}_0 & \mathbf{0} \\ \mathbf{L}_1 \mathbf{S}^{m-} & \mathbf{L}_1 \end{bmatrix} \begin{bmatrix} \mathbf{m}_0 \\ \boldsymbol{\Delta}\mathbf{m}^m \end{bmatrix} - \begin{bmatrix} \mathbf{d}_0 \\ \mathbf{d}_1 \end{bmatrix} \right\| \approx 0$$

$\mathbf{S}^{m-}$ – forward (baseline to monitor) warping
$\boldsymbol{\Delta}\mathbf{m}^m$ – time-lapse image at monitor position

Data-space inversion

$$\left\| \begin{bmatrix} \mathbf{L}_0 & \mathbf{0} \\ \mathbf{L}_1 \mathbf{S}^{m-} & \mathbf{L}_1 \mathbf{S}^{m-} \end{bmatrix} \begin{bmatrix} \mathbf{m}_0 \\ \Delta \mathbf{m}^b \end{bmatrix} - \begin{bmatrix} \mathbf{d}_0 \\ \mathbf{d}_1 \end{bmatrix} \right\| \approx 0$$

$\mathbf{S}^{m-}$ – forward (baseline to monitor) warping
$\Delta \mathbf{m}^b$ – time-lapse image at baseline position

Data-space inversion

$$\left\| \begin{bmatrix} \mathbf{L}_0 & \mathbf{0} \\ \mathbf{0} & \mathbf{U}^{\mathbf{m}-}\mathbf{L}_1^b \end{bmatrix} \begin{bmatrix} \mathbf{m}_0 \\ \mathbf{m}_1^b \end{bmatrix} - \begin{bmatrix} \mathbf{d}_0 \\ \mathbf{d}_1 \end{bmatrix} \right\| \approx 0$$

$\mathbf{U}^{m-}$ – mapping operator

$$\mathbf{U}^{m-} \approx \mathbf{L}_1 \mathbf{S}^{m-} \left[\left[(\mathbf{L}_1^b)^T \mathbf{L}_1^b \right]^{-1} (\mathbf{L}_1^b)^T \right]$$

Regularized-inversion

$$\left\| \left[\begin{array}{cc} \mathbf{L}_0 & \mathbf{0} \\ \mathbf{0} & \mathbf{U}^{\mathbf{m}-} \mathbf{L}_1^{b} \\ \hline \epsilon_0 \mathbf{R}_0 & \mathbf{0} \\ \mathbf{0} & \epsilon_1 \mathbf{R}_1 \\ \hline -\zeta_0 \mathbf{\Lambda}_0 & \zeta_1 \mathbf{\Lambda}_1 \end{array} \right] \left[\begin{array}{c} \mathbf{m}_0 \\ \mathbf{m}_1^{b} \end{array} \right] - \left[\begin{array}{c} \mathbf{d}_0 \\ \mathbf{d}_1 \\ \hline \mathbf{0} \\ \mathbf{0} \\ \hline \mathbf{0} \end{array} \right] \right\| \approx 0$$

Regularized-inversion

$$\left\| \left[\begin{array}{cc} \mathbf{L}_0 & \mathbf{0} \\ \mathbf{0} & \mathbf{U}^{\mathbf{m}-}\mathbf{L}_1^b \\ \hline \epsilon_0 \mathbf{R}_0 & \mathbf{0} \\ \mathbf{0} & \epsilon_1 \mathbf{R}_1 \\ \hline -\zeta_0 \mathbf{\Lambda}_0 & \zeta_1 \mathbf{\Lambda}_1 \end{array} \right] \left[\begin{array}{c} \mathbf{m}_0 \\ \mathbf{m}_1^b \end{array} \right] - \left[\begin{array}{c} \mathbf{d}_0 \\ \mathbf{d}_1 \\ \hline \mathbf{0} \\ \mathbf{0} \\ \hline \mathbf{0} \end{array} \right] \right\| \approx 0$$

$\mathbf{R}_i$ – spatial regularization

$\mathbf{\Lambda}_i$ – temporal regularization

ϵ_i – spatial regularization parameter

ζ_i – coupling parameter

Image-space inversion

$$\begin{bmatrix} \mathbf{H}_0 & \mathbf{0} \\ \mathbf{0} & \mathbf{H}_1^b \\ \hline \mathbf{R}_{00} & \mathbf{0} \\ \mathbf{0} & \mathbf{R}_{11}^b \\ \hline \mathbf{\Lambda}_{00} & -\mathbf{\Lambda}_{01}^b \\ -\mathbf{\Lambda}_{10}^b & \mathbf{\Lambda}_{11}^b \end{bmatrix} \begin{bmatrix} \hat{\mathbf{m}}_0 \\ \hat{\mathbf{m}}_1^b \end{bmatrix} \approx \begin{bmatrix} \tilde{\mathbf{m}}_0 \\ \tilde{\mathbf{m}}_1^b \\ \hline \mathbf{0} \\ \mathbf{0} \\ \hline \mathbf{0} \\ \mathbf{0} \end{bmatrix}$$

$\mathbf{H}_i = \mathbf{L}_i^T \mathbf{L}_i$ – Hessian
$\tilde{\mathbf{m}}_i = \mathbf{L}_i^T d_i$ – migrated image
$\hat{\mathbf{m}}_i$ – inverted image
$\mathbf{R}_{ii}$ – spatial regularization
$\mathbf{\Lambda}_{ii}$ – temporal regularization

Image-space inversion

$$\left[\begin{array}{cc} \mathbf{H}_0 & \mathbf{0} \\ \mathbf{0} & \mathbf{H}_1^b \\ \hline \mathbf{R}_{00} & \mathbf{0} \\ \mathbf{0} & \mathbf{R}_{11}^b \\ \hline \mathbf{\Lambda}_{00} & -\mathbf{\Lambda}_{01}^b \\ -\mathbf{\Lambda}_{10}^b & \mathbf{\Lambda}_{11}^b \end{array}\right] \left[\begin{array}{c} \hat{\mathbf{m}}_0 \\ \hat{\mathbf{m}}_1^b \end{array}\right] \approx \left[\begin{array}{c} \tilde{\mathbf{m}}_0 \\ \tilde{\mathbf{m}}_1^b \\ \hline \mathbf{0} \\ \mathbf{0} \\ \hline \mathbf{0} \\ \mathbf{0} \end{array}\right]$$

$\mathbf{H}$ – target-oriented approximation to the full Hessian

Image-space inversion

$$\begin{bmatrix} \mathbf{H}_0 & \mathbf{0} \\ \mathbf{0} & \mathbf{H}_1^b \\ \hline \mathbf{R}_{00} & \mathbf{0} \\ \mathbf{0} & \mathbf{R}_{11}^b \\ \hline \mathbf{\Lambda}_{00} & -\mathbf{\Lambda}_{01}^b \\ -\mathbf{\Lambda}_{10}^b & \mathbf{\Lambda}_{11}^b \end{bmatrix} \begin{bmatrix} \hat{\mathbf{m}}_0 \\ \hat{\mathbf{m}}_1^b \end{bmatrix} \approx \begin{bmatrix} \tilde{\mathbf{m}}_0 \\ \tilde{\mathbf{m}}_1^b \\ \hline \mathbf{0} \\ \mathbf{0} \\ \hline \mathbf{0} \\ \mathbf{0} \end{bmatrix}$$

$\mathbf{H}_i^b$ – Hessian with monitor geometry but baseline velocity
$\tilde{\mathbf{m}}_1^b$ – migrated monitor warped to the baseline
$\hat{\mathbf{m}}_1^b$ – inverted monitor a the baseline postion

Image-space inversion

$$\begin{bmatrix} \mathbf{H}_0 & \mathbf{0} \\ \mathbf{0} & \mathbf{H}_1^b \\ \hline \mathbf{R}_{00} & \mathbf{0} \\ \mathbf{0} & \mathbf{R}_{11}^b \\ \hline \mathbf{\Lambda}_{00} & -\mathbf{\Lambda}_{01}^b \\ -\mathbf{\Lambda}_{10}^b & \mathbf{\Lambda}_{11}^b \end{bmatrix} \begin{bmatrix} \hat{\mathbf{m}}_0 \\ \hat{\mathbf{m}}_1^b \end{bmatrix} \approx \begin{bmatrix} \tilde{\mathbf{m}}_0 \\ \tilde{\mathbf{m}}_1^b \\ \hline \mathbf{0} \\ \mathbf{0} \\ \hline \mathbf{0} \\ \mathbf{0} \end{bmatrix}$$

Data-fitting

Image-space inversion

$$\left[\begin{array}{cc} \mathbf{H}_0 & \mathbf{0} \\ \mathbf{0} & \mathbf{H}_1^b \\ \hline \mathbf{R}_{00} & \mathbf{0} \\ \mathbf{0} & \mathbf{R}_{11}^b \\ \hline \mathbf{\Lambda}_{00} & -\mathbf{\Lambda}_{01}^b \\ -\mathbf{\Lambda}_{10}^b & \mathbf{\Lambda}_{11}^b \end{array}\right] \left[\begin{array}{c} \hat{\mathbf{m}}_0 \\ \hat{\mathbf{m}}_1^b \end{array}\right] \approx \left[\begin{array}{c} \tilde{\mathbf{m}}_0 \\ \tilde{\mathbf{m}}_1^b \\ \hline \mathbf{0} \\ \mathbf{0} \\ \hline \mathbf{0} \\ \mathbf{0} \end{array}\right]$$

Spatial regularization – non-stationary dip-filtering
Temporal regularization – difference operator

Image-space inversion

$$\begin{bmatrix} \mathbf{H}_0 & \mathbf{0} \\ \mathbf{0} & \mathbf{H}_1^b \\ \hline \mathbf{R}_{00} & \mathbf{0} \\ \mathbf{0} & \mathbf{R}_{11}^b \\ \hline \mathbf{\Lambda}_{00} & -\mathbf{\Lambda}_{01}^b \\ -\mathbf{\Lambda}_{10}^b & \mathbf{\Lambda}_{11}^b \end{bmatrix} \begin{bmatrix} \hat{\mathbf{m}}_0 \\ \hat{\mathbf{m}}_1^b \end{bmatrix} \approx \begin{bmatrix} \tilde{\mathbf{m}}_0 \\ \tilde{\mathbf{m}}_1^b \\ \hline \mathbf{0} \\ \mathbf{0} \\ \hline \mathbf{0} \\ \mathbf{0} \end{bmatrix}$$

– Can be easily extended to multiple surveys

Image-space inversion

$$\left[\begin{array}{cc} \mathbf{H}_0 & \mathbf{0} \\ \mathbf{0} & \mathbf{H}_1^b \\ \hline \mathbf{R}_{00} & \mathbf{0} \\ \mathbf{0} & \mathbf{R}_{11}^b \\ \hline \mathbf{\Lambda}_{00} & -\mathbf{\Lambda}_{01}^b \\ -\mathbf{\Lambda}_{10}^b & \mathbf{\Lambda}_{11}^b \end{array}\right] \left[\begin{array}{c} \hat{\mathbf{m}}_0 \\ \hat{\mathbf{m}}_1^b \end{array}\right] \approx \left[\begin{array}{c} \tilde{\mathbf{m}}_0 \\ \tilde{\mathbf{m}}_1^b \\ \hline \mathbf{0} \\ \mathbf{0} \\ \hline \mathbf{0} \\ \mathbf{0} \end{array}\right]$$

– Can be easily extended to multiple surveys
– Can be solved in a target-oriented way (e.g., around the reservoir)

Image-space inversion

$$\begin{bmatrix} \mathbf{H}_0 & \mathbf{0} \\ \mathbf{0} & \mathbf{H}_1^b \\ \hline \mathbf{R}_{00} & \mathbf{0} \\ \mathbf{0} & \mathbf{R}_{11}^b \\ \hline \mathbf{\Lambda}_{00} & -\mathbf{\Lambda}_{01}^b \\ -\mathbf{\Lambda}_{10}^b & \mathbf{\Lambda}_{11}^b \end{bmatrix} \begin{bmatrix} \hat{\mathbf{m}}_0 \\ \hat{\mathbf{m}}_1^b \end{bmatrix} \approx \begin{bmatrix} \tilde{\mathbf{m}}_0 \\ \tilde{\mathbf{m}}_1^b \\ \hline \mathbf{0} \\ \mathbf{0} \\ \hline \mathbf{0} \\ \mathbf{0} \end{bmatrix}$$

– Can be easily extended to multiple surveys
– Can be solved in a target-oriented way (e.g., around the reservoir)
– Can be efficiently repeated with different regularization parameters

Image-space inversion

$$\left[\begin{array}{cc} \mathbf{H}_0 & \mathbf{0} \\ \mathbf{0} & \mathbf{H}_1^b \\ \hline \mathbf{R}_{00} & \mathbf{0} \\ \mathbf{0} & \mathbf{R}_{11}^b \\ \hline \mathbf{\Lambda}_{00} & -\mathbf{\Lambda}_{01}^b \\ -\mathbf{\Lambda}_{10}^b & \mathbf{\Lambda}_{11}^b \end{array}\right] \left[\begin{array}{c} \hat{\mathbf{m}}_0 \\ \hat{\mathbf{m}}_1^b \end{array}\right] \approx \left[\begin{array}{c} \tilde{\mathbf{m}}_0 \\ \tilde{\mathbf{m}}_1^b \\ \hline \mathbf{0} \\ \mathbf{0} \\ \hline \mathbf{0} \\ \mathbf{0} \end{array}\right]$$

– Can be easily extended to multiple surveys
– Can be solved in a target-oriented way (e.g., around the reservoir)
– Can be efficiently repeated with different regularization parameters
– Can be easily integrated with *conventional* inversion framework

Location: Norwegian North Sea

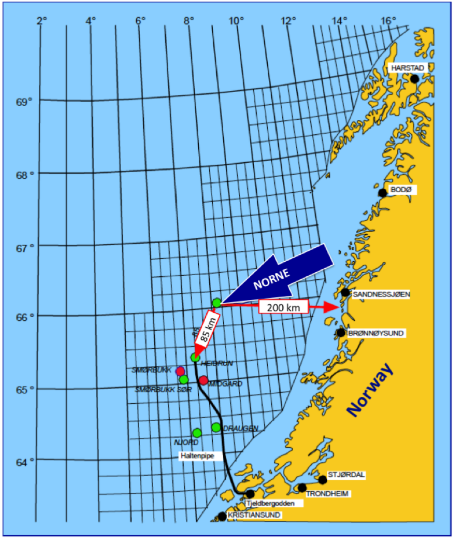

Modified from: STATOIL Annual Report (2006)

gayeni@sep.stanford.edu

Baseline: stacked image/velocity model

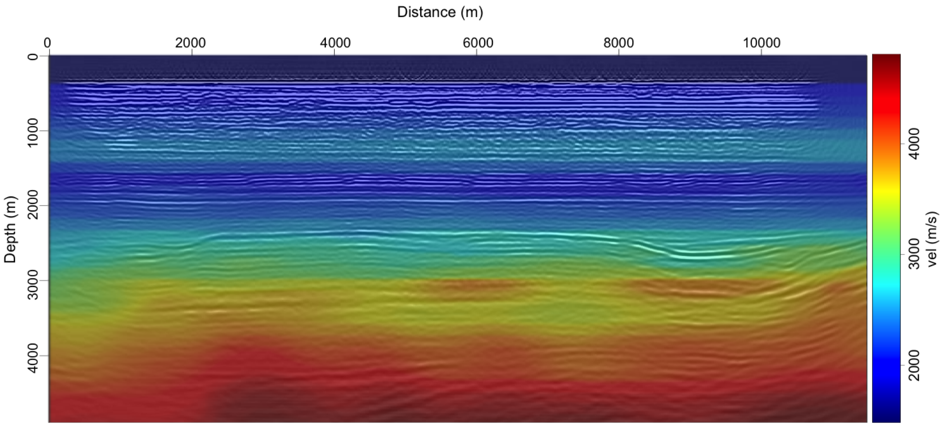

Baseline – Target area

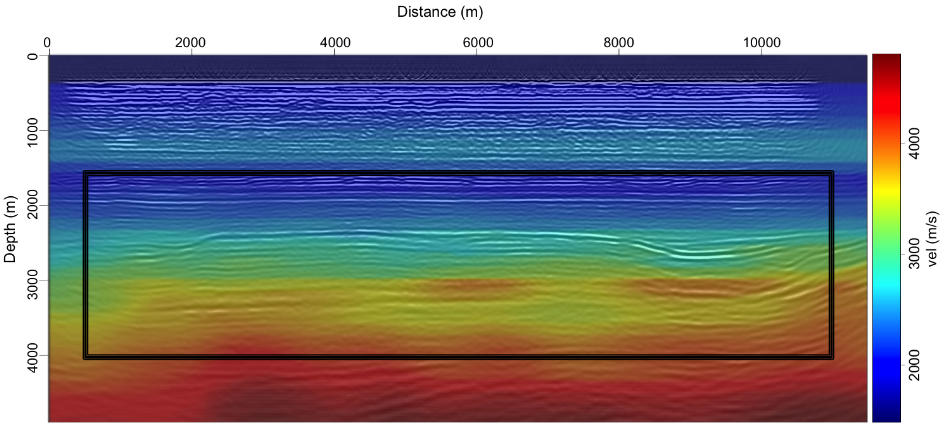

Baseline – Target area

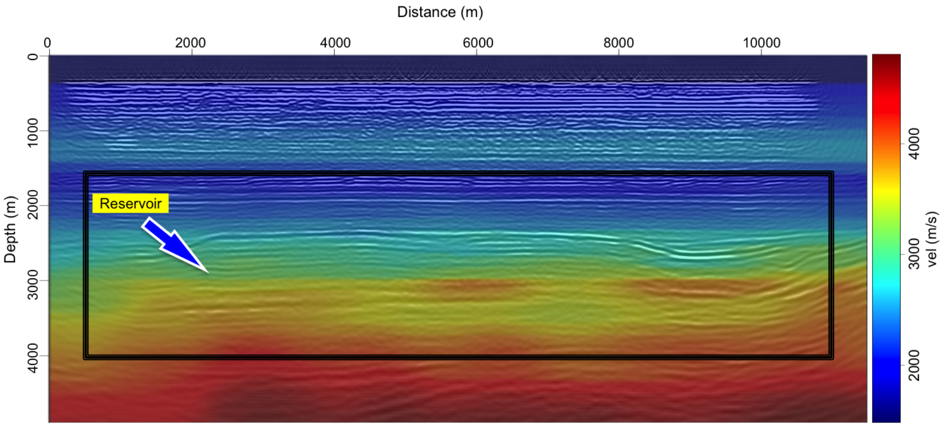

Baseline – Target area

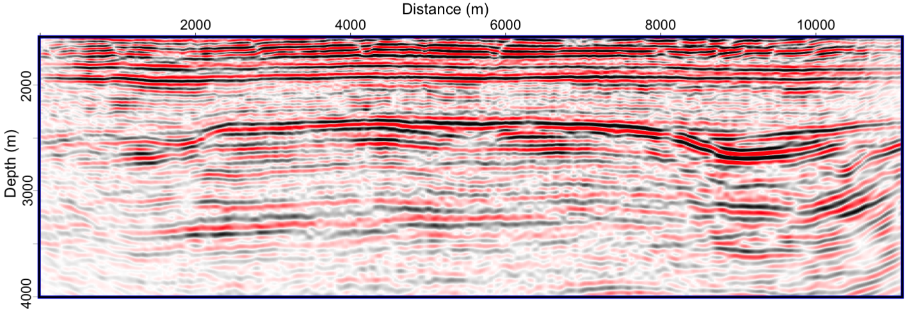

gayeni@sep.stanford.edu

Baseline: Raw

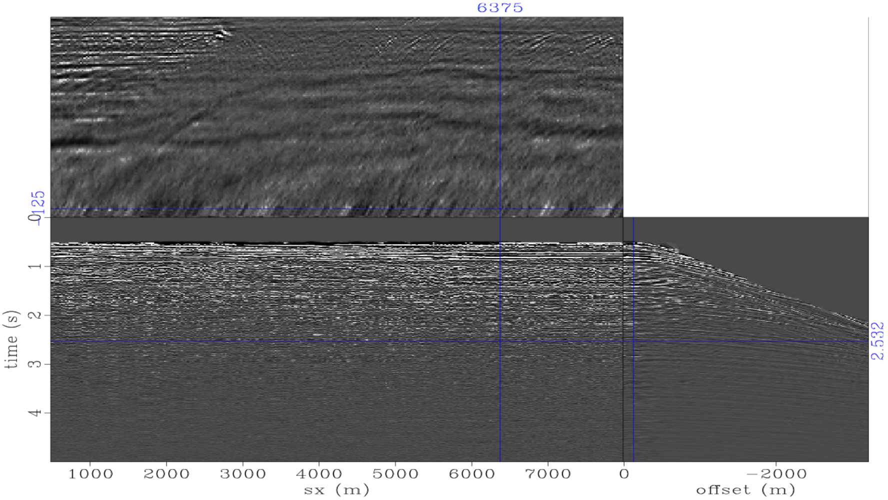

Baseline: After demultiple

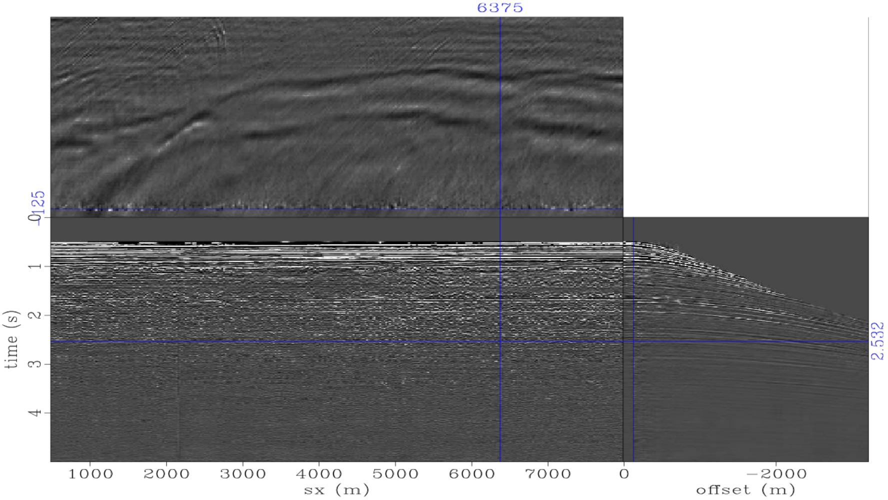

Baseline: Radon model

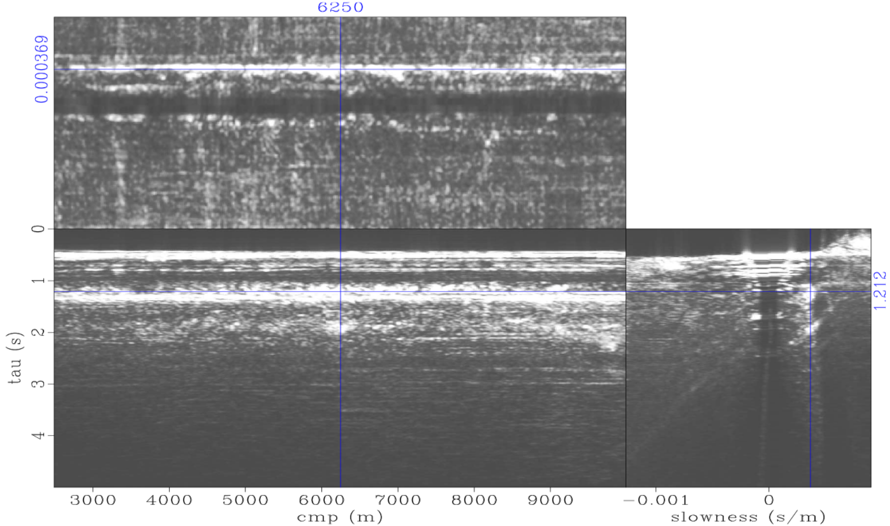

gayeni@sep.stanford.edu

Baseline: Radon model

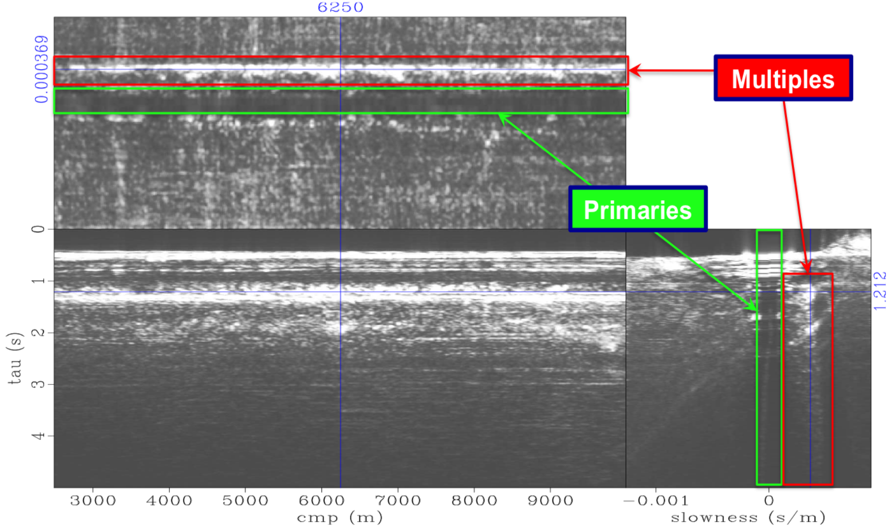

gayeni@sep.stanford.edu

Baseline: Prestack image before processing

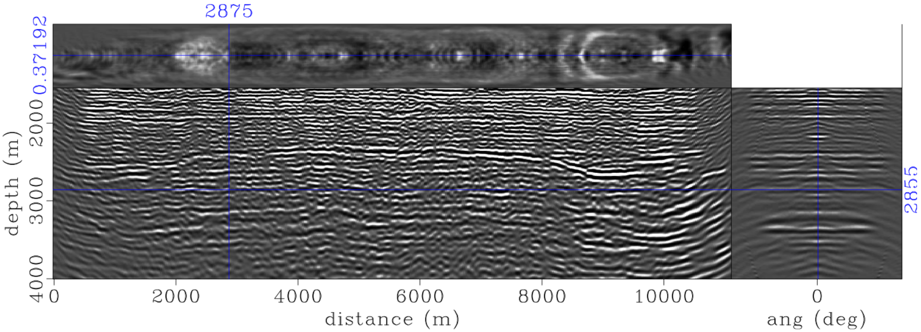

Baseline: Prestack image after processing

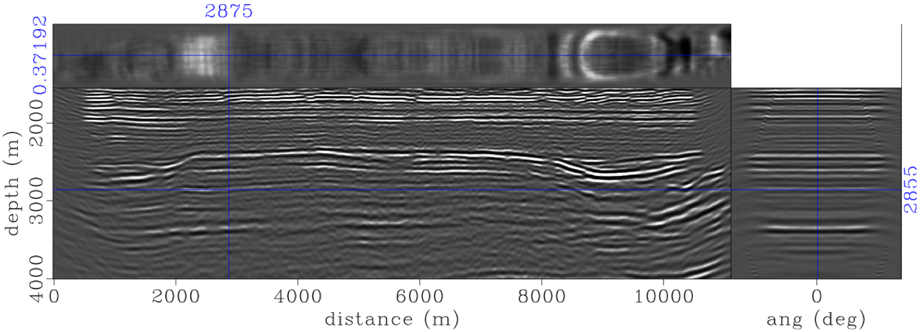

Time-lapse image: raw

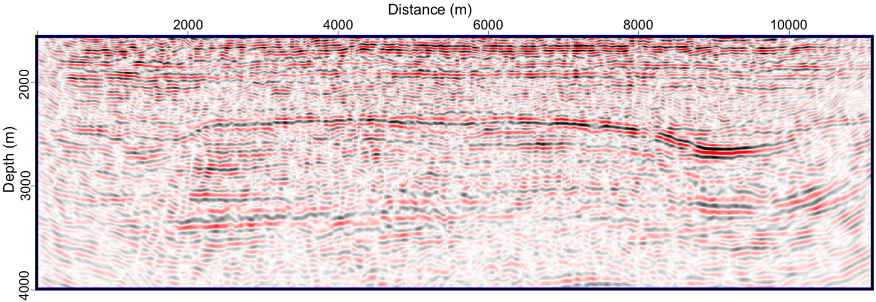

gayeni@sep.stanford.edu

Time-lapse image: demultiple

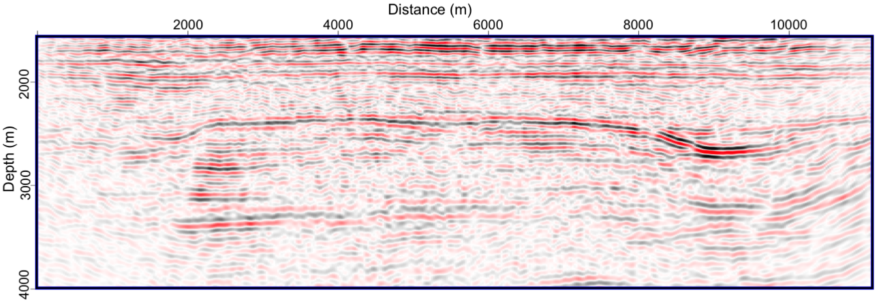

Time-lapse image: amplitude correction

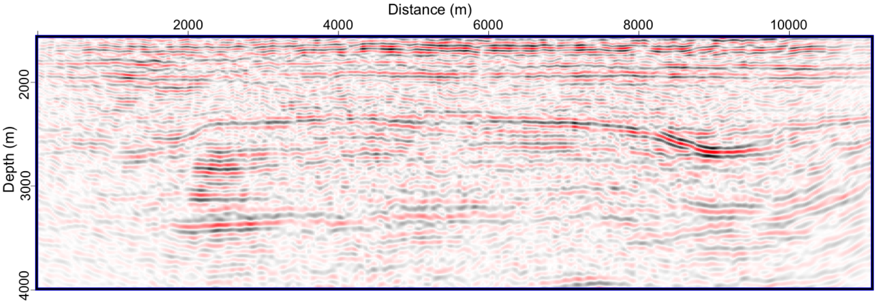

gayeni@sep.stanford.edu

Time-lapse image: warping (prestack+ poststack)

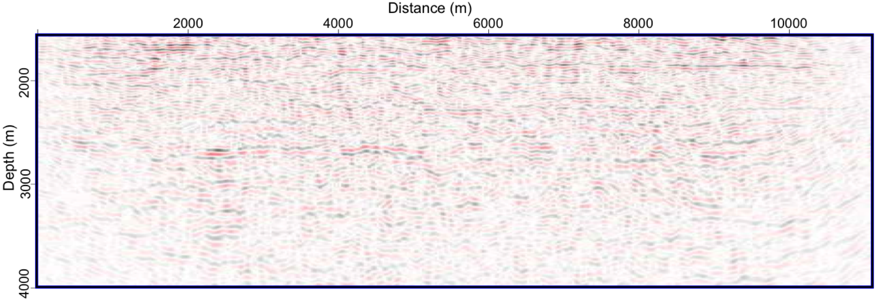

Time-lapse image: inversion

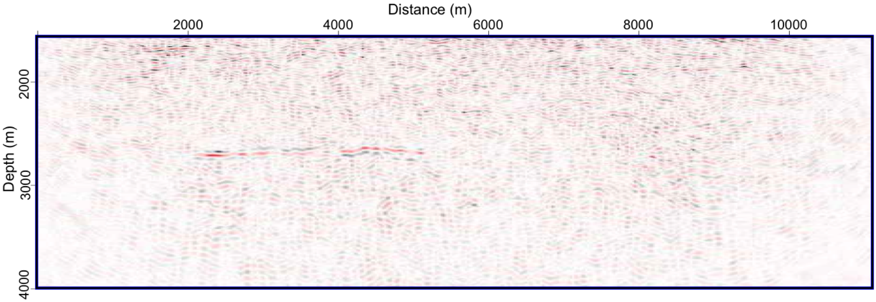

Time-lapse image: inversion

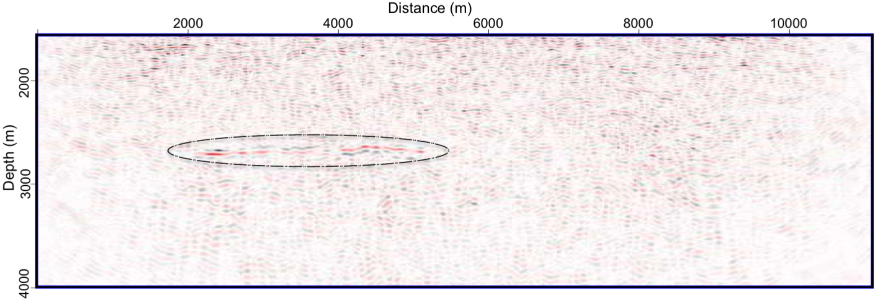

Time-lapse image: inversion

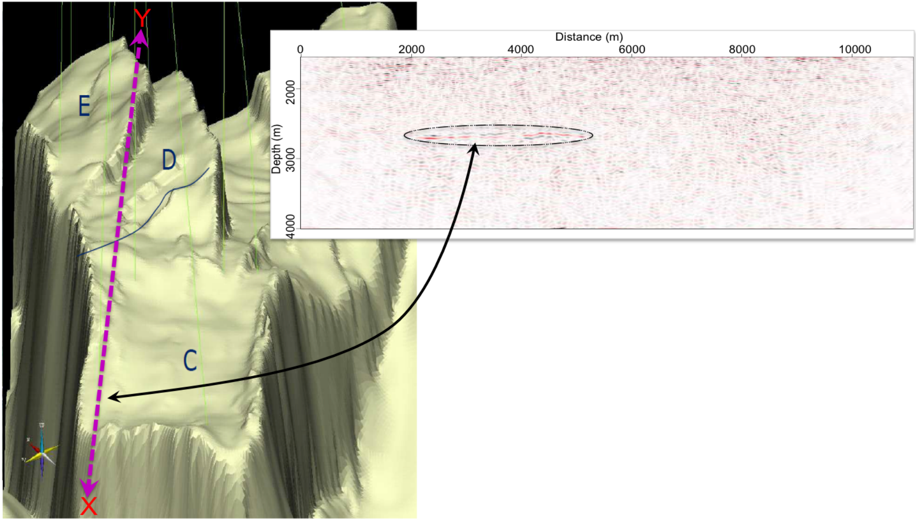

Time-lapse image: inversion

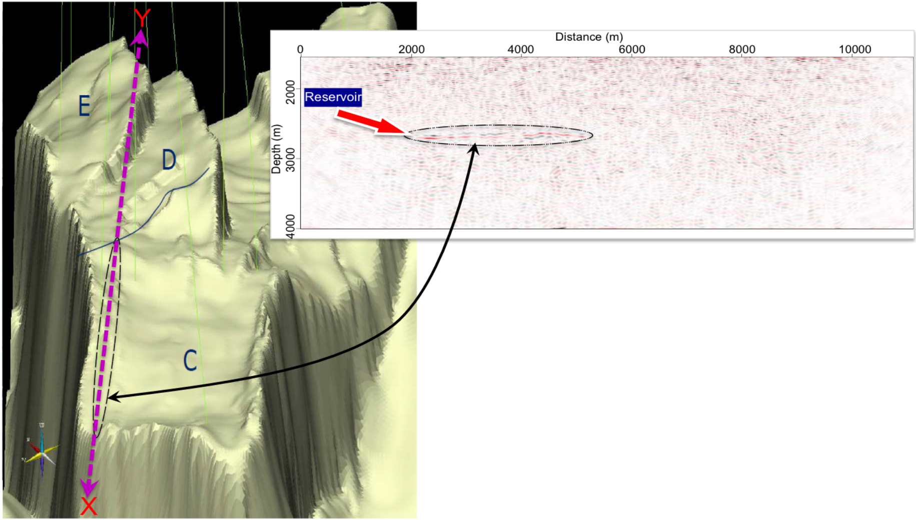

Time-lapse image: inversion

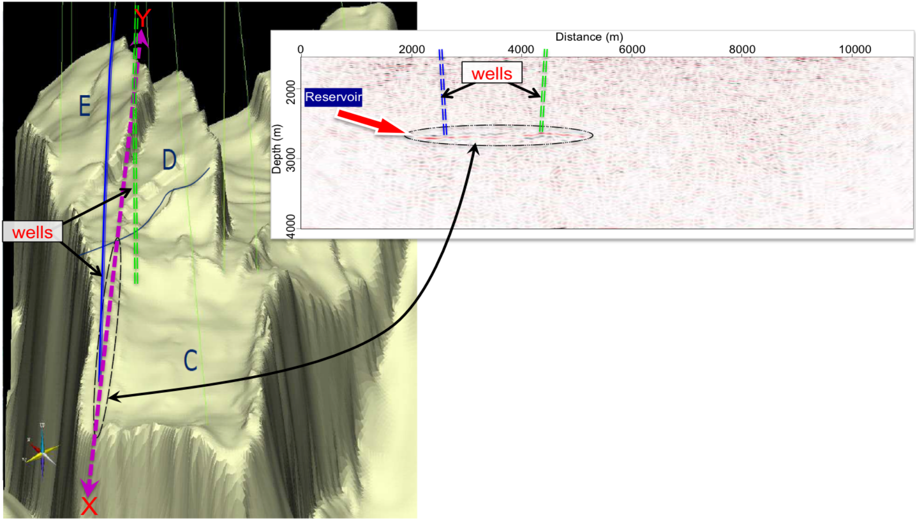

Time-lapse requires careful processing/interpretation!

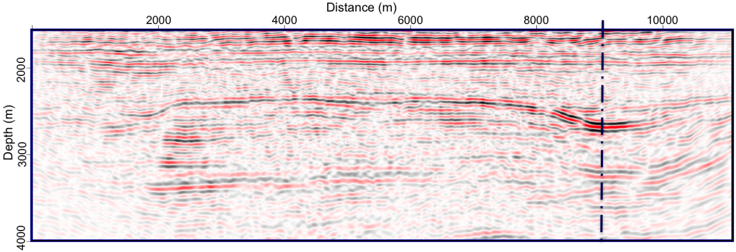

Raw time-lapse – Artifacts

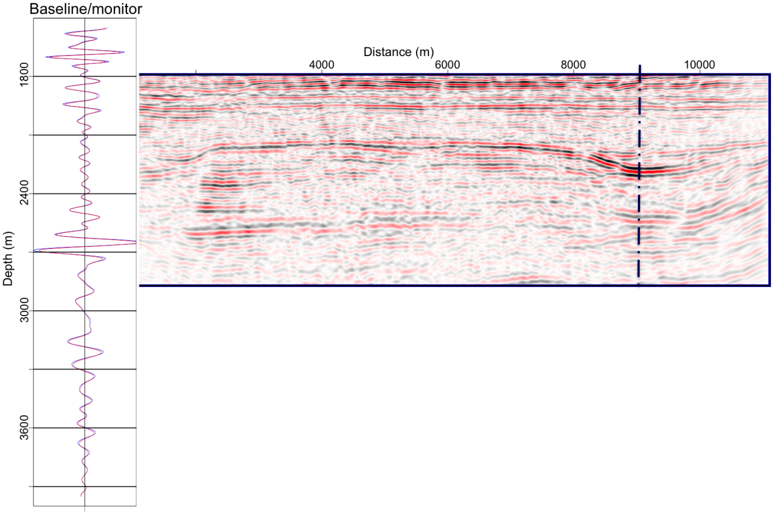

Raw time-lapse – Artifacts

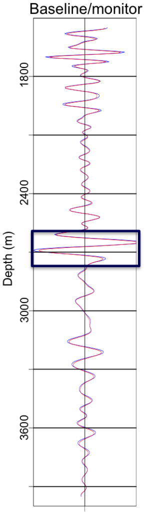

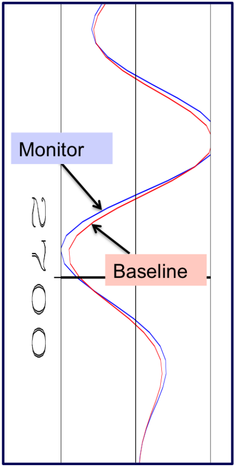

gayeni@sep.stanford.edu

After multiple attenuation

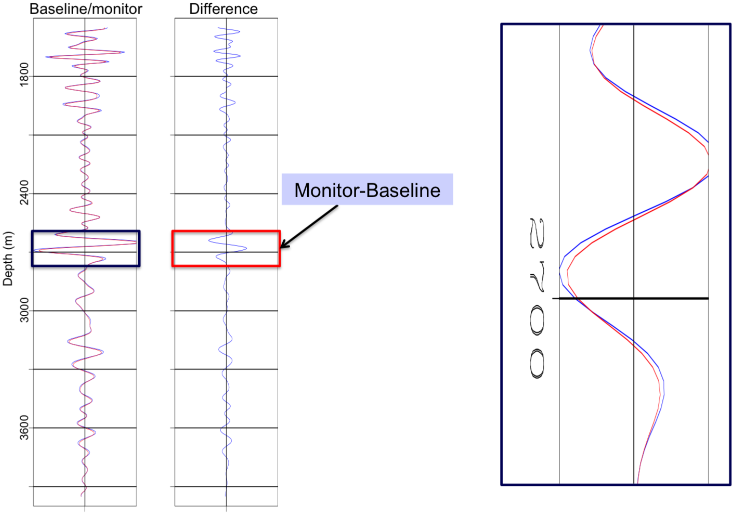

After amplitude balancing

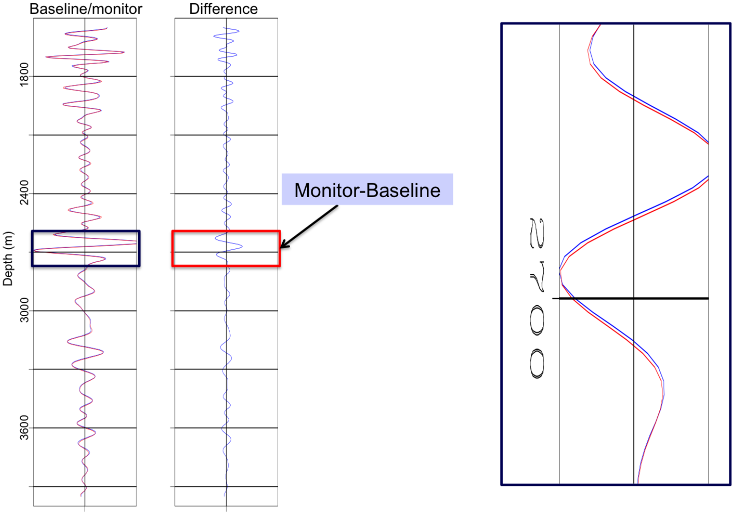

After warping

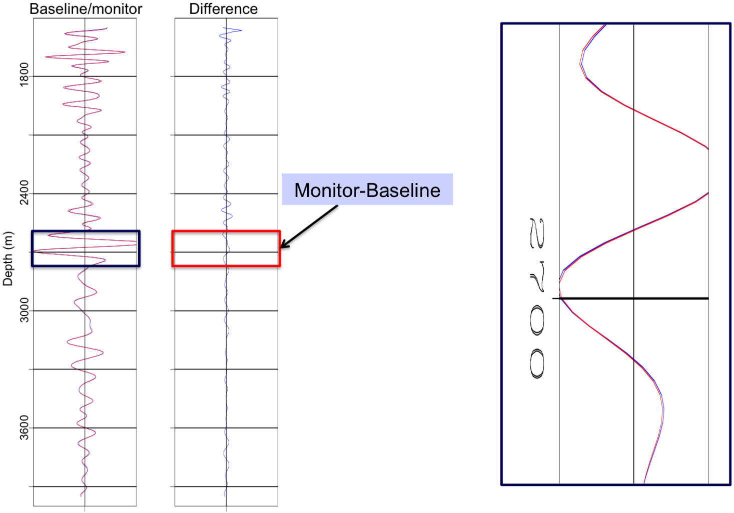

After warping

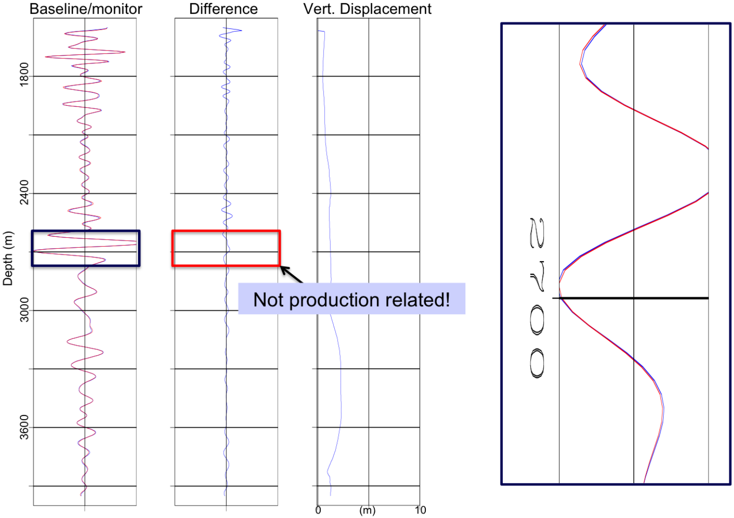

Raw time-lapse – Reservoir

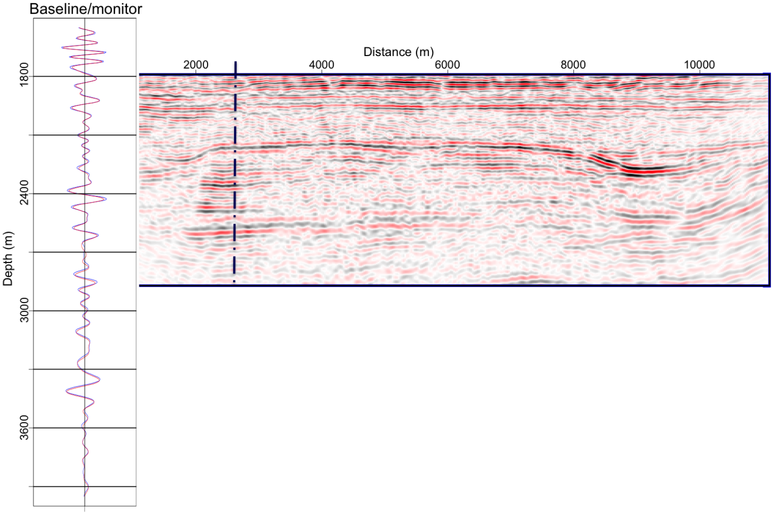

After multiple attenuation

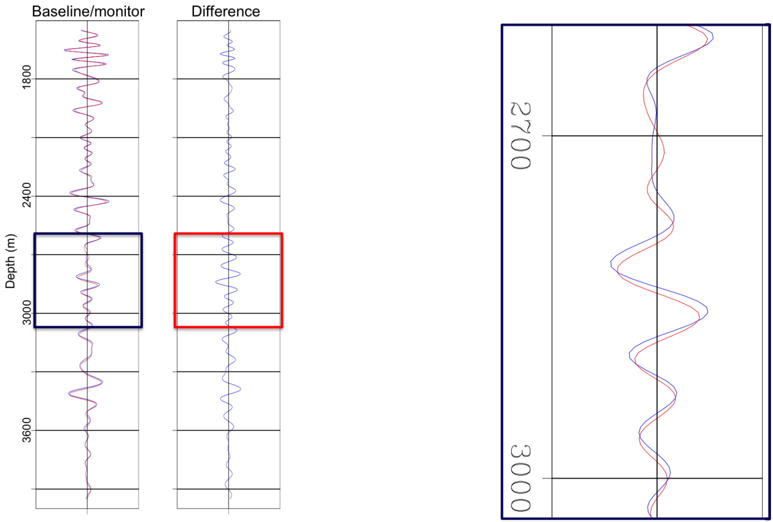

gayeni@sep.stanford.edu

After amplitude balancing

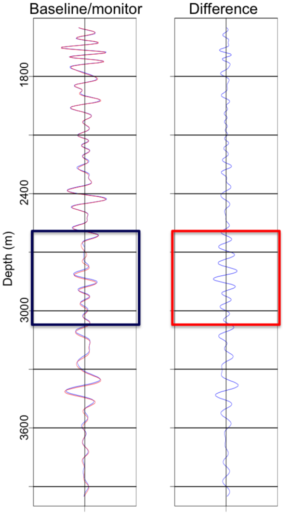

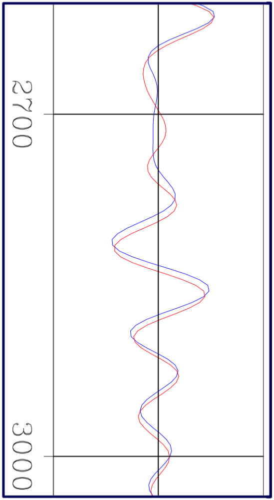

After warping

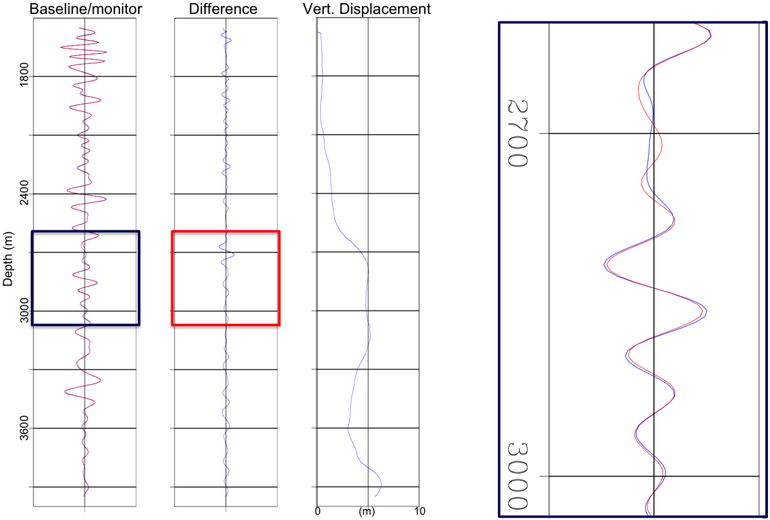

After warping

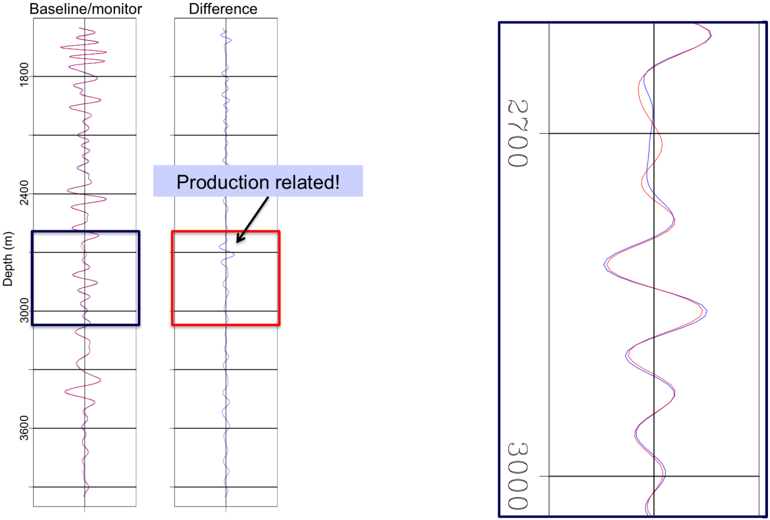

gayeni@sep.stanford.edu

After warping

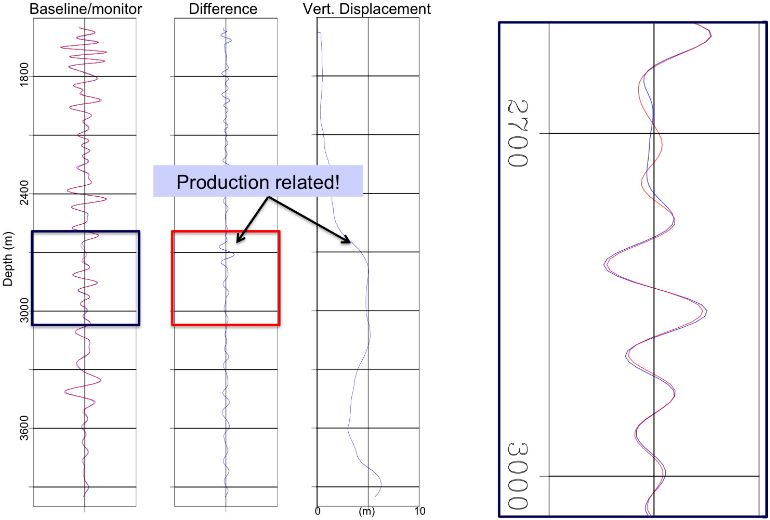

gayeni@sep.stanford.edu

After warping

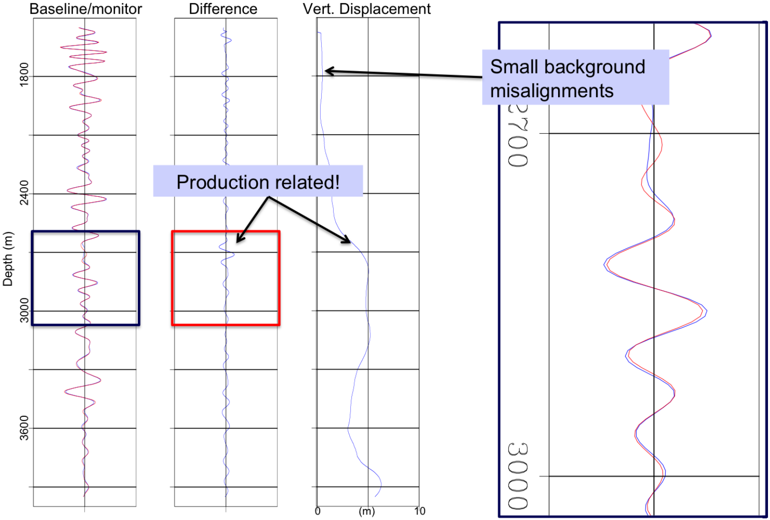

Complete baseline

Baseline

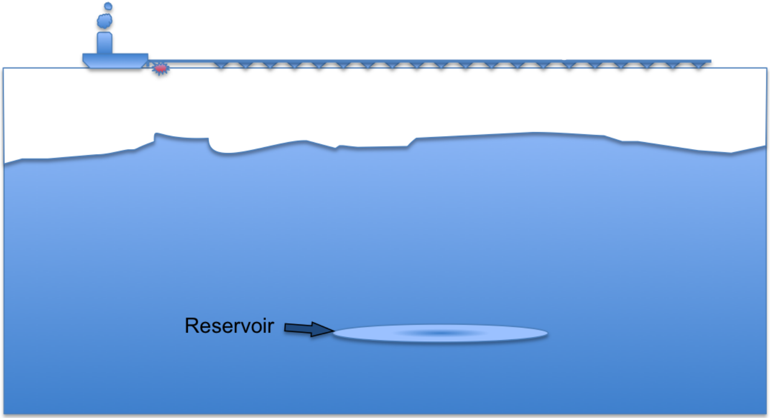

Gapped monitor

Monitor

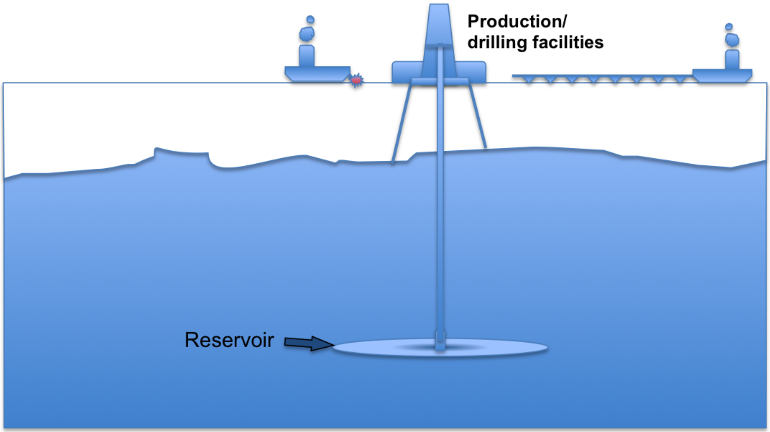

Data: Complete baseline

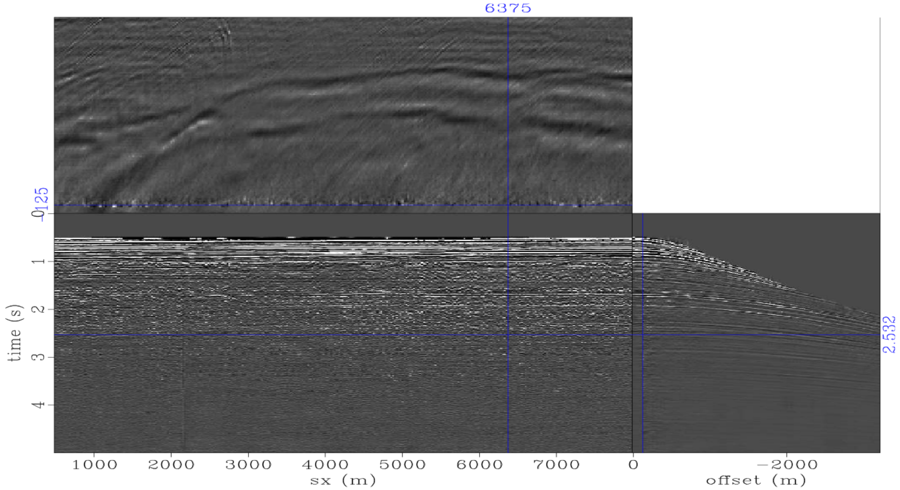

gayeni@sep.stanford.edu

Data: Gapped monitor

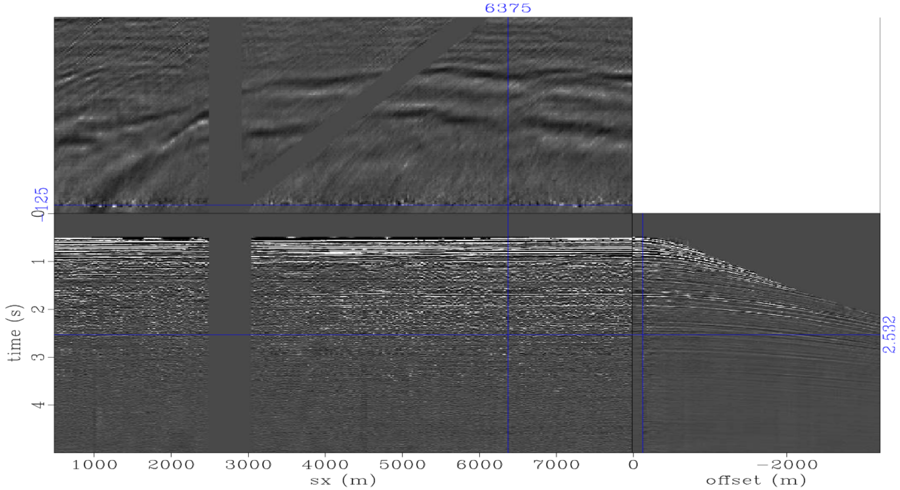

Data: Gapped monitor

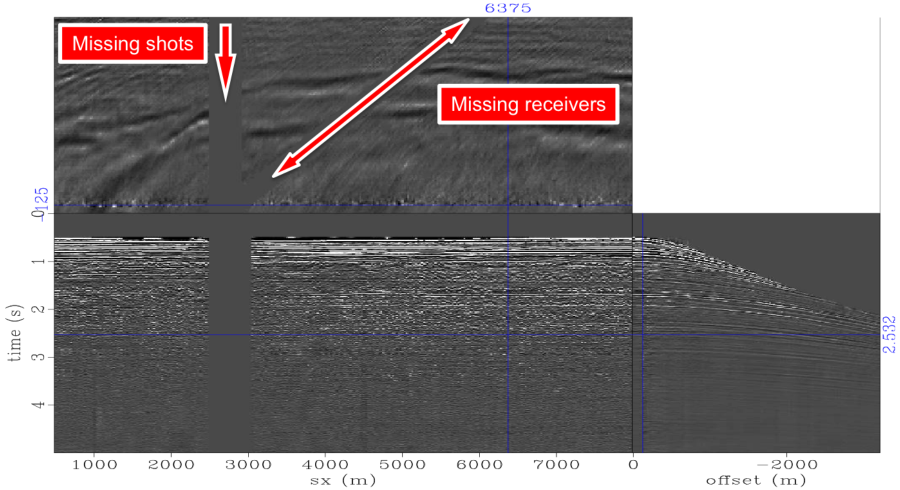

Illumination ratio: monitor/base

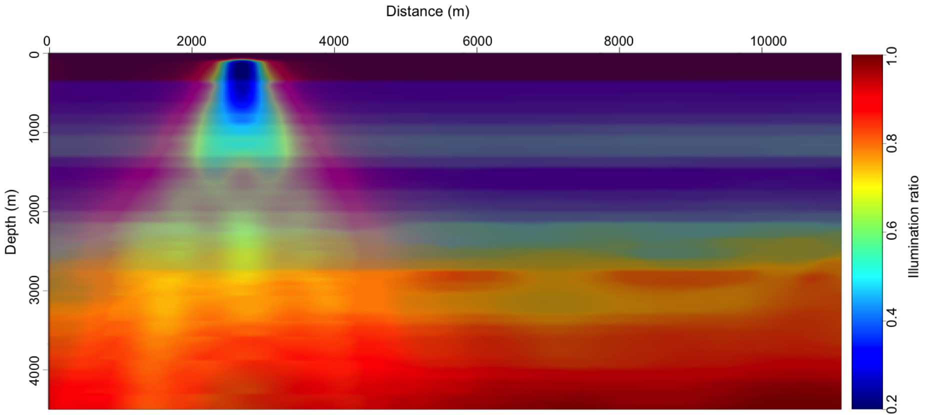

Illumination ratio: monitor/base

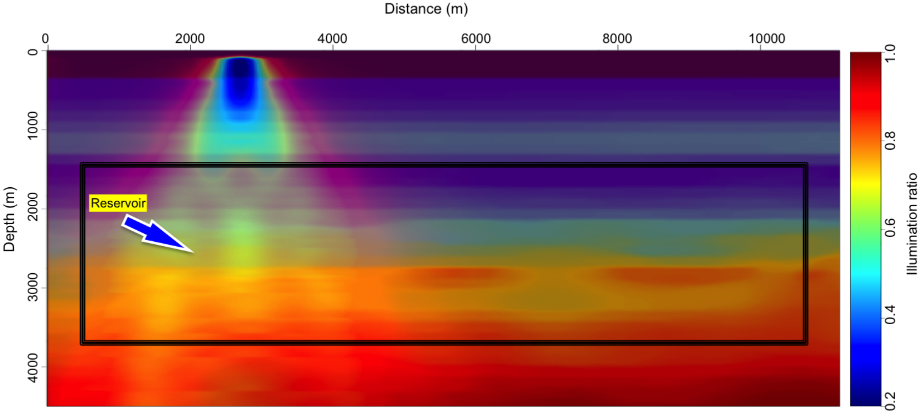

Illumination ratio: monitor/base

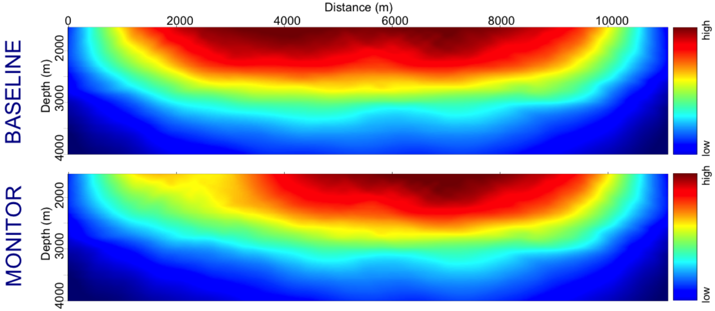

Illumination ratio: monitor/base

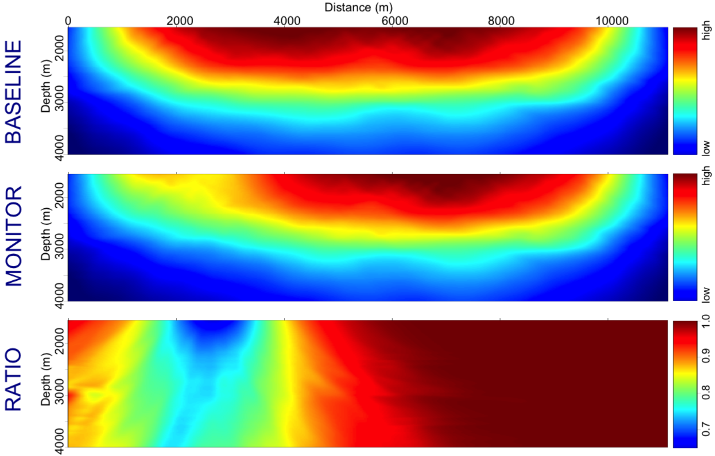

Illumination ratio: monitor/base

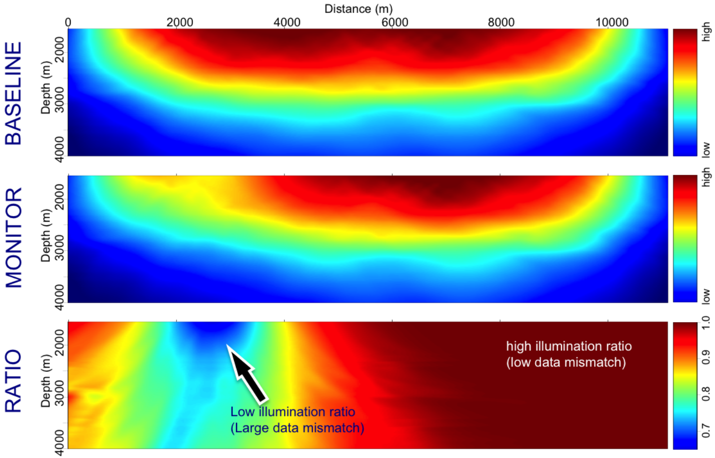

Illumination ratio: monitor/base

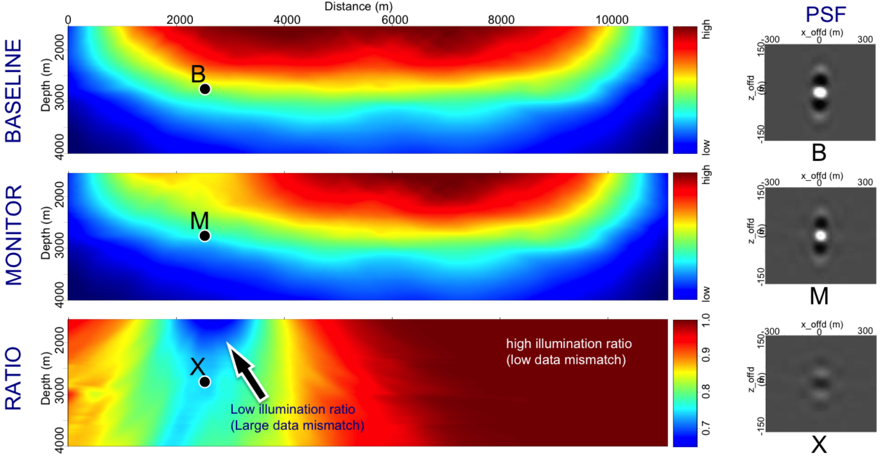

Illumination ratio: monitor/base

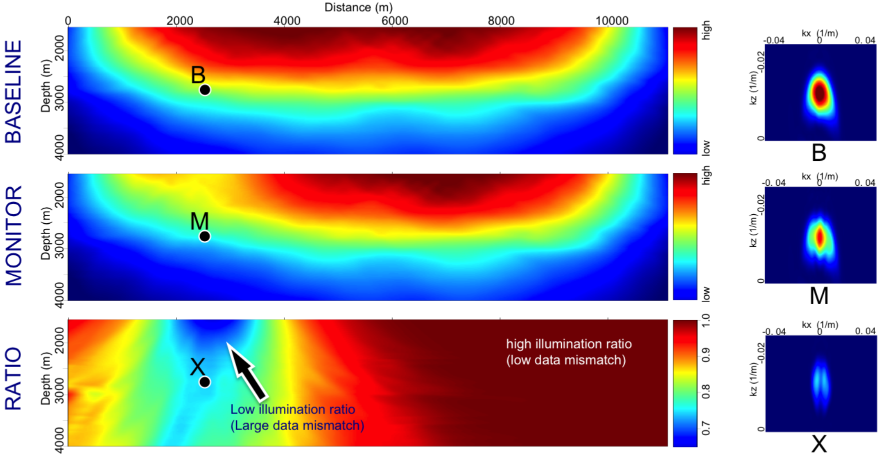

gayeni@sep.stanford.edu

Prestack warping: vertical components

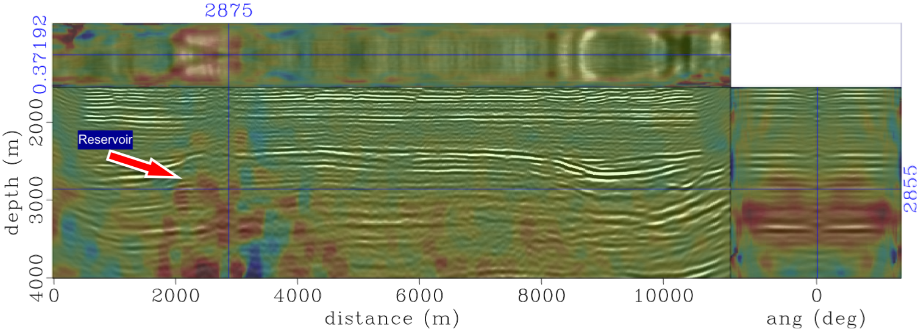

Prestack warping: before

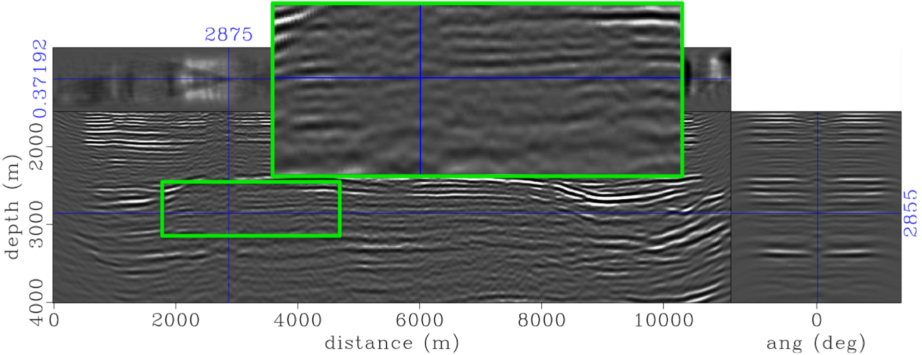

gayeni@sep.stanford.edu

Prestack warping: after

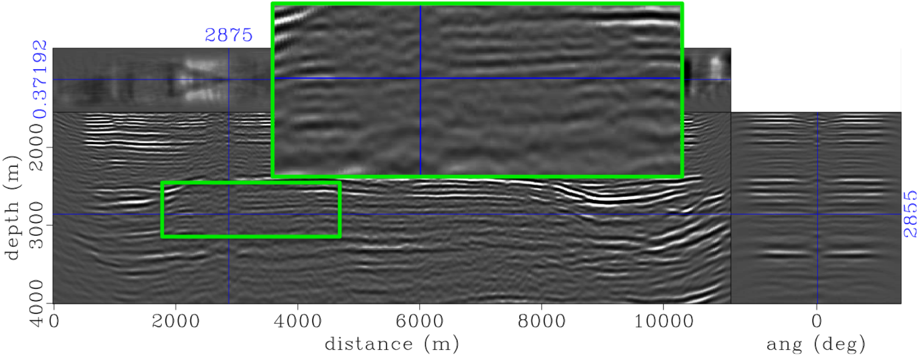

Prestack warping: before

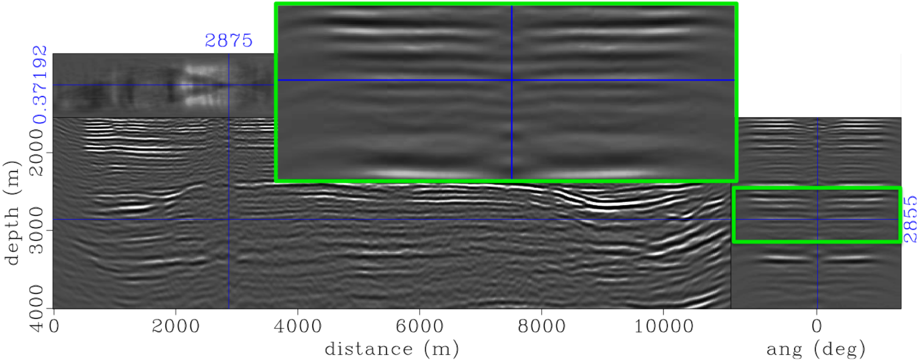

Prestack warping: after

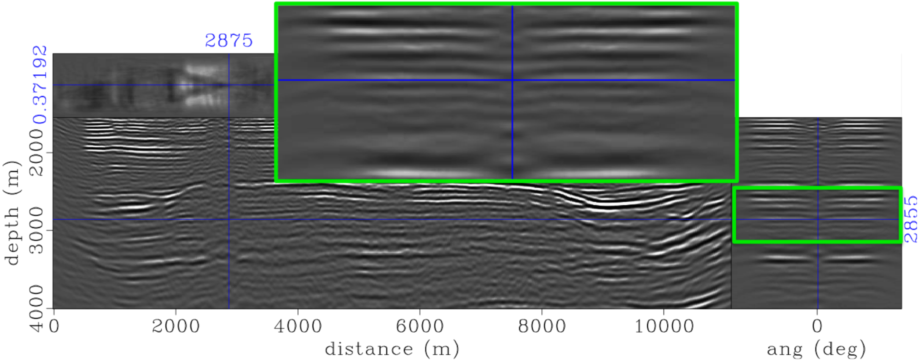

Time-lapse image: raw (complete data)

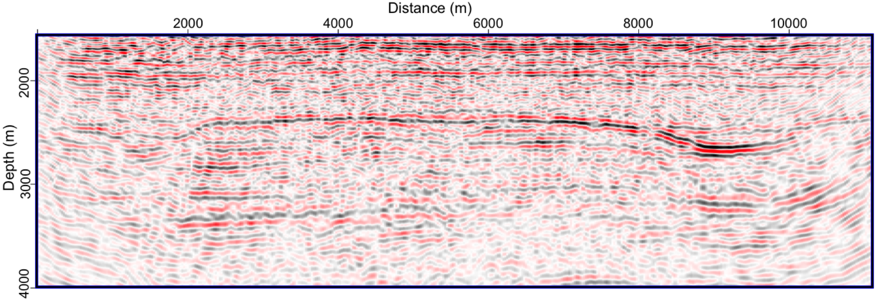

Time-lapse image: raw (gapped data)

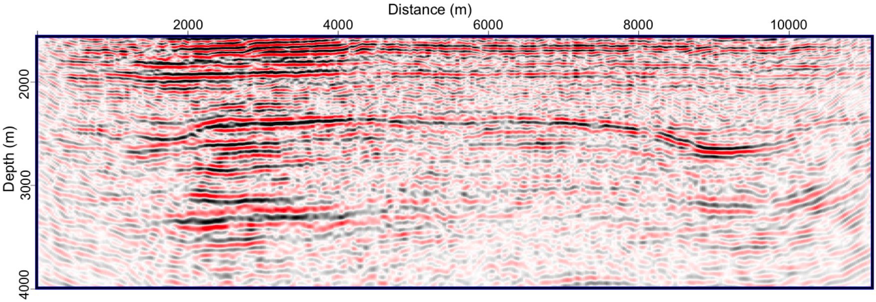

gayeni@sep.stanford.edu

Time-lapse image: after all processing (gapped data)

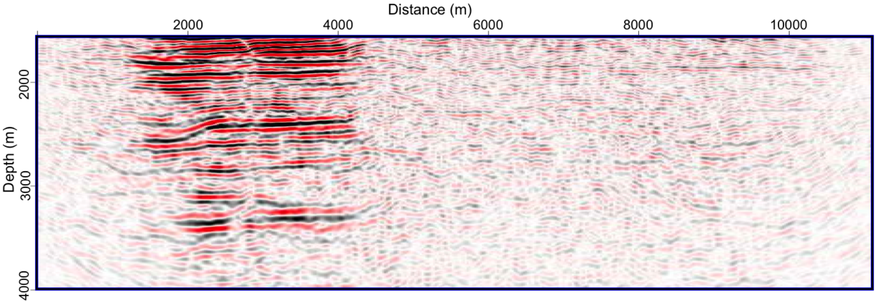

Time-lapse image: after WE inversion (gapped data)

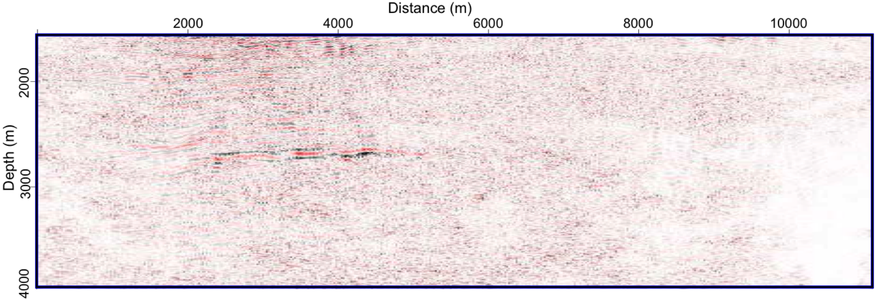

Time-lapse image: raw (gapped data)

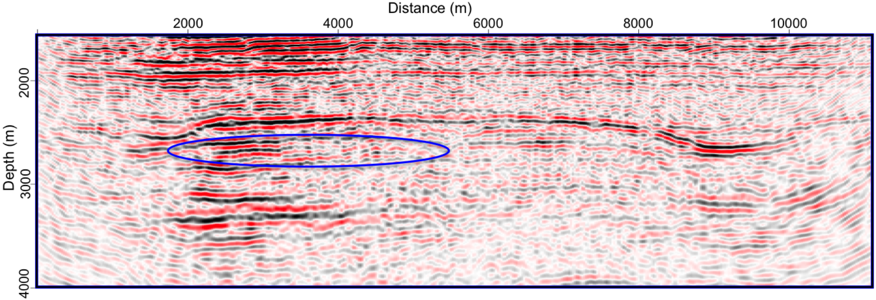

Time-lapse image: after WE inversion (gapped data)

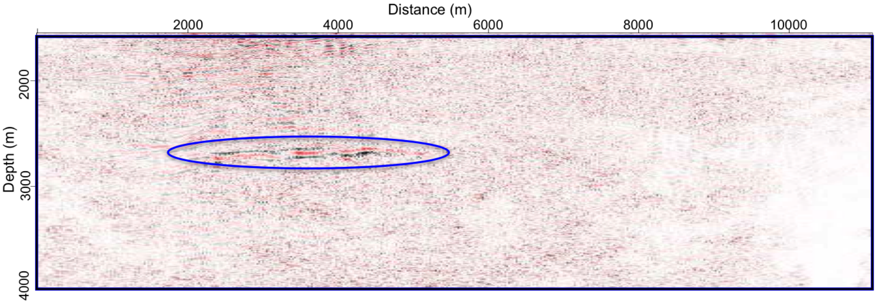

gayeni@sep.stanford.edu

Conclusions

- Time-lapse seismic data sets can be more accurately imaged using joint wave-equation inversion
- Careful data processing is required before inversion or before any meaningful interpretation of time-lapse amplitude differences

gayeni@sep.stanford.edu

Conclusions

- Time-lapse seismic data sets can be more accurately imaged using joint wave-equation inversion
- Careful data processing is required before inversion or before any meaningful interpretation of time-lapse amplitude differences
- We demonstrated that wave-equation inversion provides improved results over conventional time-lapse processing

Conclusions

- Time-lapse seismic data sets can be more accurately imaged using joint wave-equation inversion
- Careful data processing is required before inversion or before any meaningful interpretation of time-lapse amplitude differences
- We demonstrated that wave-equation inversion provides improved results over conventional time-lapse processing
- Finally, we showed that wave-equation inversion can attenuate artifacts caused by inconsistent acquisition geometries between surveys

Conclusions

- Time-lapse seismic data sets can be more accurately imaged using joint wave-equation inversion
- Careful data processing is required before inversion or before any meaningful interpretation of time-lapse amplitude differences
- We demonstrated that wave-equation inversion provides improved results over conventional time-lapse processing
- Finally, we showed that wave-equation inversion can attenuate artifacts caused by inconsistent acquisition geometries between surveys

gayeni@sep.stanford.edu

Acknowledgements

- We thank Statoil and partners (ENI and Petoro) for donating the data sets through the NTNU/IO CENTRE.
- We thank the Stanford Center for Computational Earth & Environmental Science for providing the computer resources used in this study.

Ongoing work

- Application to full-azimuth 3D time-lapse data set

Thanks

STANFORD EXPLORATION PROJECT